Published in final edited form as:
Opt Lett. 2010 December 1; 35(23): 3889–3891.

On the potential for molecular imaging with Cerenkov luminescence

Matthew A. Lewis[*], **Vikram D. Kodibagkar**, **Orhan K. Öz**, and **Ralph P. Mason**
Advanced Radiological Sciences, Department of Radiology, UT Southwestern Medical Center at Dallas, 5323 Harry Hines Blvd, Dallas, TX, 75390-9058

Abstract

Recent observation of optical luminescence due to beta decay from suitable radiotracers has led to the possible development of new preclinical optical imaging methods. The generation of photons that can be detected using instrumentation optimized for bioluminescence imaging has been putatively associated with the Cerenkov effect. We describe the simultaneous utilization of fluorescence reporters to convert the Cerenkov luminescence to longer wavelengths for better tissue penetration and also for modulating the luminescence spectrum for potential molecular imaging strategies.

Planar bioluminescence imaging (BLI) and bioluminescent tomography (BLT) are important research tools in the preclinical imaging armamentarium. From a technical perspective, the challenge of bioluminescence, chemiluminescence, or Cerenkov luminescence imaging is to effectively detect the small number of optical photons that escape the surface of the animal. Recently, Robertson et al. reported the optical imaging of positron emitters and described the optical signals as being *consistent with Cerenkov radiation* [1]. Similar optical signals were reported soon thereafter in microfluidic chips designed for ^{18}F radio-synthesis. Cho et al. reported a minimum detectable activity of 0.16 μCi/mm^2, with no intervening materials or tissues to attenuate the Cerenkov luminescence [2]. Translation from *in vitro* to *in vivo* imaging was described in [1,3], with comparison and fusion for microCT and microPET. Multispectral imaging of optical photons produced by both ^{18}F and ^{68}Ga as a function of organ location, tissue attenuation, and depth, opening the possibility of metabolic and dynamic imaging [4,5]. In all cases, the existing instrumentation and image reconstruction methods for bioluminescence tomography are well-suited for Cerenkov luminescence tomography (CLT), so rapid development of this modality is anticipated.

We note that optical imaging has previously been used to determine positron range in a water-equivalent phantom. Hasegawa et al. recently reported imaging a plastic scintillator with a small well for ^{18}F using a film camera with exposure up to 5 minutes [6]. After beta decay, a positron will progressively lose its kinetic energy through multiple scattering with the media. In a scintillating medium, this energy can be converted to the generation of optical photons. In some cases, fluorescent materials will similarly respond to the introduction of a charged particle emitter, generating visible light photons either through the transfer of energy during beta particle scattering or through excitation via a Cerenkov photon intermediary.

[*]Corresponding author: Matthew.Lewis@UTSouthwestern.edu.

OCIS codes: 170.3880, 170.2655, 260.3800.

There remains some controversy as to the mechanism of light production due to beta decay. Most of the cited literature includes a figure demonstrating *in vitro* data in line with the theoretical $1/\lambda^2$ dependence of Cerenkov radiation [1,2,4,5,7]. While it is clear from this data that Cerenkov radiation is the probable mechanism *in vitro*, there are some reports of light production that are inconsistent with the conditions for Cerenkov production from lower energy beta particles [5] or alpha particles [8]. In addition, recent work by Liu et al. also indicates that beta decay can stimulate quantum dot fluorescence [7]. It is conceivable that this process can be exploited to develop new molecular imaging strategies that allow simultaneous probing of multiple targets.

In this Letter, we describe experiments to investigate the cross-talk between Cerenkov luminescence and fluorescent agents. In particular, we focus not only on the ability of fluorophores to convert the optical signal to longer wavelengths with better tissue penetration, but on the definitive changes in the luminescence spectrum that occur when the radionuclide and fluorophore are co-located. It is this molecular signaling method that we find offers the greatest potential for new imaging techniques.

Fluorine-18 is not the ideal radioisotope for Cerenkov luminescence. While positron kinetic energy should be minimized for PET resolution, larger positron kinetic energies produce more Cerenkov photons. Nevertheless, ^{18}F is commonly available, and we obtained 1 mCi calibrated ^{18}FDG in 60 μl syringes (PETNET Solutions, Inc., Dallas, TX). All optical imaging was performed on the Xenogen IVIS Spectrum (Caliper Life Sciences, Hopkinton, MA) in the UT Southwestern Small Animal Imaging Resource (SW-SAIR) using black anodized aluminum or black plastic well plates. In previous bioluminescence research, we have noted that some plastic well plates possess significant phophorescence, and there is some concern that beta emission could also excite these optical emission mechanisms.

To investigate luminescence associated with a fluorophore, we prepared a 38 mM solution of fluorescein in 0.1 N NaOH. The solution was diluted into 4 equal volumes in a black plastic well plate in a $4{:}2{:}1{:}\frac{2}{3}$ ratio (5.4 mM, 2.7 mM, 1.3 mM, 0.9 mM). Above micromolar concentrations, fluorescein suffers from autoquenching. When imaged in fluorescent mode (0.1s exposure, F/4, no binning, 465nm excitation), the wells exhibited nearly identical light emission due to the severe autoquenching (data not shown). An additional 10 μL solution containing 9.7 μCi of ^{18}FDG was then pipetted into each well, including a fifth control well with no fluorophore. The well plate was then imaged in luminescence mode (60s exposure, F/1, 4×4 binning). As seen in Figure 1, the luminescence image is correlated with the fluorophore concentration, despite the autoquenching. In all wells, the luminescence is brighter than that produced by the positron emitter alone. The focal points of light in empty well 5 are specular reflections of the broadband light source for the bright-field background image. Direct gamma-ray interactions with the CCD sensor do not appear to be problematic for this modality.

Next, the experiment was repeated using emission filters in 20 nm steps between 500 and 700 nm. For maximum sensitivity, the optical stage in the Xenogen system was set to minimize the field-of-view, and the camera settings from the previous experiment were maintained. As shown in Figure 2, the observed luminescence is several orders of magnitude less than the fluorescence emission achievable with optical excitation, and we observe a subtle shift toward longer wavelengths for the luminescence spectrum compared to the fluorescence spectrum.

Furthermore, we investigated the luminescence of other fluorophores with potential pre-clinical application. Solutions for europium (III) chloride hexahydrate (480 mM, Aldrich),

thulium (III) chloride hexahydrate (380 mM, Aldrich), gadolinium (III) chloride hexahyrdate (390 mM, Aldrich), indocyanine green (42 mM, Aldrich), and gadopentetate dimuglumine (469.01 mg/mL, Magnevist, Bayer HealthCare Pharmaceuticals) were added to a black plastic well plate with 14 μCi ^{18}F per well. These agents span the range of fluorescence. Gadolinium salts and solutions have fluorescence excitation and emission in the ultraviolet [9,10], while ICG has excitation and emission peaks in the near infrared that are highly dependent upon both concentration and the solvent properties [11]. In all cases, each well exhibited more luminescence due to positron emission than a well with ^{18}FDG alone (data not shown), although no spectral peaks were observed except for fluoroscein and the lanthanide discussed below.

The only remarkable spectrum from a signaling standpoint is from the europium solution. This is not surprising since the transformation of MR contrast agent to optical contrast agents by the replacement of Gd with Eu is well-described in the literature [12]. As shown in Figure 3, the europium solution exhibits a clear luminescence peak near 600 nm. In addition, a strong second peak is observed near 700 nm, which is more ideal for imaging in tissue. Although the europium fluorescence sprectrum is complex and highly dependent upon the required chelation complex, we note that some proposed imaging agents (such as EuPCTA-$(gly)_3$) maintain a strong fluorescence peak at 700 nm [13]. When activity-matched ^{74}As ($T_{\frac{1}{2}}$ = 18 days) is substituted for ^{18}F, increased luminescence is uniformly observed due to the higher energy beta particles (max. energies: β− 1.36 MeV, β+ 1,54 MeV). We note that the first luminescence peak for the europium solution appears to be red-shifted with ^{74}As excitation compared to ^{18}F. The 700 nm peak for europium excited in the presence of ^{18}F is also comparable in magnitude to the 600 nm peak, which is not consistent with the expected decrease in intensity for higher total angular momentum (J) states. We also evaluated the IRDye 800CW 2-DG optical probe (LICOR Biosciences, Lincoln, NE) reconstituted according to manufacturer's protocol. With ^{74}As, an unexpected subtle peak was observed at 580–600 nm. With ^{18}F, some enhanced luminescence above 800 nm was also noted, consistent with the expected fluorescence properties of the agent. For these multispectral imaging experiments, 300 s exposures were used for each 20 nm filter band, and the ^{18}FDG-derived data is time-corrected for the expected radioactive decay during the acquisition time. Due to the 20 nm spectral bands, some features of the luminescence spectra may be unobservable, but this could remedied by using a spectrofluorometer with a low dark current detector.

For positron annihilation gamma rays, the attenuation coefficient at 511 keV for the $EuCl_3$ solution is indistinguishable from water or soft tissue [14]. Since the mean free path of a typical 511 keV photon in this case (10 cm) is much larger than the sample dimensions, most annihilation gammas will exit without interacting with the fluorophore. However, we observed a well containing only fluorophore but surrounded by wells containing ^{74}As to exhibit 53% more luminescence than background from an empty well. This observation is presumably due to lower energy photons from the complicated ^{74}As decay scheme interacting with the sample. This effect is negligible however compared to the luminescence associated with beta emission and a co-located fluorophore.

One could exploit the addition of the fluorophore solely as a tool to improve the transmission of the Cerenkov luminescence in small animal imaging. However, with long-lived isotopes such as ^{89}Zr and ^{74}As, one can envision other improvements provided by the beta emitting isotope. For example, in fluorescence molecular tomography (FMT), the excitation is typically a known excitation source on the surface of the animal. With Cerenkov light imaging, the excitation source is the distribution of radioisotope, which may also be unknown. In this case, a joint estimation image reconstruction problem is required.

However, it is also possible that the radioisotope distribution may be known from a separate nuclear medicine imaging study.

In addition to modifying the optical imaging reconstruction problem, we also envision molecular imaging strategies where the radioisotope and optical agent target different biological moieties. With a long-lived isotope and long biological half-life for the radiolabelled agent, one could return at later times to target with multiple optical imaging agents. If the radiotracer and optical agent label the same tissue, then the Cerenkov luminescence emission detected on the animal surface will be modulated with the types of spectral signatures described in this Letter. To develop these methods *in vivo* even in a preclinical model will require optimization of the radioisotope decay parameters (beta kinetic energy, decay modes, etc.), the targeted radiotracer, the targeted fluorescent agent, the flourescence emission spectrum, and the image reconstruction and estimation methods. On the instrumentation side, the existing hardware for BLI is fairly well-matched for Cerenkov imaging. Significant improvement in the optical coupling efficiency between the surface of last scattering on the animal surface and the high sensitivity sensor is needed, given the poor efficiency of lens coupling. The ideal Cerenkov light sensor may be a high sensitivity, integrating detector that can be placed in contact with the animal skin, much like an ultrasound transducer.

Acknowledgments

This work was supported by National Institutes of Health (NIH) grants U24 CA126608 and 1S10RR024757-01, Department of Defense CDMRP BCRP W81XWH-06-1-0475, and the Cain Foundation. We are grateful to Dr. A. Hermanne at the University of Brussels for providing ^{74}As and to Dr. Guiyang Hao for its purification.

References

1. Robertson R, Germanos MS, Li C, Mitchell GS, Cherry SR, Silva MD. Phys. Med. Biol 2009;54:N355. [PubMed: 19636082]
2. Cho JS, Taschereau R, Olma S, Liu K, Chen Y-C, Shen CK-F, van Dam RM, Chatziioannou AF. Phys. Med. Biol 2009;54:6757. [PubMed: 19847018]
3. Li C, Mitchell GS, Cherry SR. Opt. Lett 2010;35:1109. [PubMed: 20364233]
4. Spinelli AE, D'Ambrosio D, Calderan L, Marengo M, Sbarbati A, Boschi F. Phys. Med. Biol 2010;55:483. [PubMed: 20023328]
5. Liu H, Zhang X, Xing B, Han P, Gambhir SS, Cheng Z. Small 2010;6:1087. [PubMed: 20473988]
6. Hasegawa T, Yoshida E, Shibuya K, Murayama H. Med. Phys 2009;36:402. [PubMed: 19291979]
7. Liu H, Ren G, Miao Z, Zhang X, Tang X, Han P, Gambhir SS, Cheng Z. PLoS One 2010;5:e9470. [PubMed: 20208993]
8. Ruggiero A, Holland JP, Lewis JS, Grimm J. J. Nucl. Med 2010;51:1123. [PubMed: 20554722]
9. Dieke GH, Leopold L. J. Opt. Soc. Am 1957;47:944.
10. Bertam-Berg A, Mainka E, Ache HJ. Fresenius Z. Anal. Chem 1989;333:766.
11. Yuan B, Chen N, Zhu Q. J. Biomed. Opt 2004;9:497. [PubMed: 15189087]
12. Manning HC, Goebel T, Thompson RC, Price RR, Lee H, Bornhop DJ. Bioconjugate Chem 2004;15:1488.
13. Rojas-Quijano FA, Benjo ET, Tircso G, Kalman FK, Baranyai Z, Aime S, Sherry AD, Kovacs Z. Chem. Eur. J 2009;15:13188.
14. Nowotny R. IAEA-NDS-195. 1998

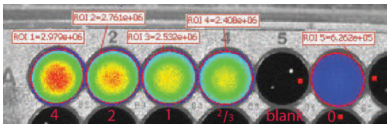

Fig. 1.

Dependence of luminescence in $4{:}2{:}1{:}\frac{2}{3}$ auto-quenching solutions of fluorescein compared to background ^{18}FDG Cerenkov luminescence.

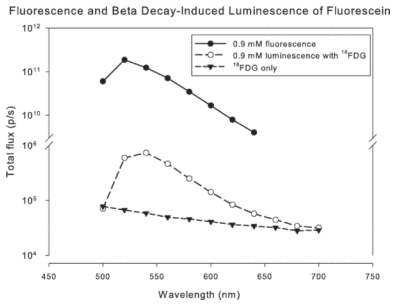

Fig. 2.
Comparison of fluorescein fluorescence and luminescence associated with beta decay.

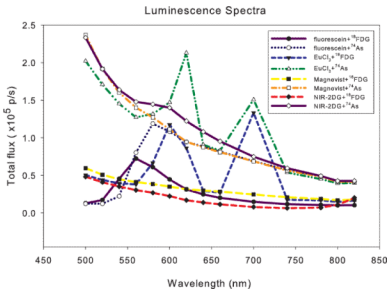

Fig. 3.
Luminescence of select fluorescent agents due to ^{18}F and ^{74}As beta emission.